Engineering Science and Technology, an International Journal 24 (2021) 911–924

HOSTED BY

ELSEVIER

Contents lists available at ScienceDirect

Engineering Science and Technology, an International Journal

journal homepage: www.elsevier.com/locate/jestch

A novel approach for optimal placement and sizing of active power filters in radial distribution system with nonlinear distributed generation using adaptive grey wolf optimizer

Ashokkumar Lakum, Vasundhara Mahajan *

Electrical Engineering Department, Sardar Vallabhbhai National Institute of Technology, Surat 395007, India

ARTICLE INFO

Article history:
Received 25 April 2020
Revised 8 October 2020
Accepted 14 January 2021
Available online 27 February 2021

Keywords:
Active power filter
Adaptive grey wolf optimizer
Distributed generation
Power quality
Radial distribution system

ABSTRACT

This paper presents the optimal placement and sizing (OPAS) of active power filter (APF) considering photovoltaic distributed generation (PVDG) and nonlinear load to control the harmonics as per IEEE-519 standard limits. For the varying nature of PVDG output, the injection of harmonics into the distribution system is thoroughly investigated by incorporating hourly solar irradiance data. In this paper, a novel extended nonlinear load position based APF current injection (ENLPCI) technique is proposed to find the number of APFs and optimal buses for placement of APFs. The optimal placement for APF is calculated here for three distinct cases: a) only one state for minimum number of APFs, b) more than one state with different total harmonic distortion in voltage (THDv) with the same number of APFs and c) more than one state with the same THDv with the same number of APFs. The size and cost of APF are calculated and compared using grey wolf optimization (GWO) and its adaptive version (AGWO) algorithms for each hour. Further, the ENLPCI is also validated by GWO and AGWO algorithms for the optimal results. The proposed algorithm is tested on the IEEE-69 bus test system. The results show that the variation of solar irradiance remarkably affects the OPAS of APF. The AGWO performed better compared to GWO to find the optimal cost of APF.

1. Introduction

Distribution generation (DG) is one of the main components of a smart grid. This concept is the backbone of the modern power system. It has gained the wide publicity due to its advantages like; enhancement of voltage profile, improvement in security and reliability, increase in energy efficiency by reducing power loss [1,2]. It is categorized into two parts (i) sources which comprise of fossil fuel and (ii) renewable energy sources (RES). Fuel cells, IC engines, and turbines are included in the first type of DG. Photovoltaic and wind power generators are the prime RES [3,4].

The integration of RES based DGs in the radial distribution system (RDS) is a crucial task. To get the qualitative benefits, the appropriate integration is required [5–7]. It has disadvantages like; intermittent availability, available only in the day, etc. Improper integration of DG results in power quality problems. The prime source of harmonics is a converter [8] and a converter based DG injects harmonics into the RDS, it is considered as a nonlinear DG (NLDG) [8–10]. It increases the individual harmonics distortion in voltage (IHDv) as well as the total harmonic distortion in voltage (THDv) in RDS.

As per the IEEE standard 519, THDv and IHDv should be less than 5% and 3%, respectively [11]. To achieve this standard, the control of harmonics is essential. Passive and active harmonic filters can be employed to reduce the harmonics. Though passive filters are cost- effective and simple in construction/operation, they have a problem of resonance with the impedance of RDS and it has fixed compensation. Moreover, if the harmonic spectrum contains a wide range of harmonics, passive filters become bulky [12]. To overcome these disadvantages, active power filters (APF) are used [13]. To mitigate the harmonics in RDS, the simple solution is to place APFs at all nonlinear load buses with their current rating equal to that of the corresponding nonlinear load. But it is highly expensive and therefore, an optimization technique is required [14] for the placement, sizing, and cost of APF.

In the existing literature, genetic algorithm, particle swarm optimization, and its variants, firefly algorithm, harmony search algorithm, trade-off risk analysis method, and grey wolf optimizer

* Corresponding author.
E-mail addresses: aclakum@gmail.com (A. Lakum), vasu.daygood@gmail.com (V. Mahajan).

Peer review under responsibility of Karabuk University.

https://doi.org/10.1016/j.jestch.2021.01.011
2215-0986/

(GWO) algorithms have been implemented to solve optimal placement and sizing (OPAS) of APF [14–23].

In the above-cited studies, the researchers have not considered the variable harmonic level during the day as expected. The nonlinear load in the RDS is variable in nature hence the harmonics also vary with time, which is more effective when NLDG is used. The output power of NLDG is varying with solar irradiance, which gradually increases till the noon and then gradually decreases from the noon to the evening. Therefore, the output power, as well as the harmonics, are more at noon compared to morning and evening hours.

In [24], the results showed the significance of time-varying load in analyzing the PV penetration in RDS. It has been noted that the power quality indicators are severely affected by new load patterns in [25] ignoring the time-varying load which may result in a nonoptimal solution. According to the noteworthy effect of variable harmonics injection into the RDS by NLDG and nonlinear load, this variation must be included in the analysis. In this situation, to decide the number of APF, its placement, size, and cost for each hour is a tough task. To simulate the real problem, from hour 6 to hour 19 the hourly output of NLDG is taken, and the nonlinear load is connected according to the output of NLDG.

The various indices have been used for optimal placement and sizing for different devices. In [26], the most candidate buses for installing capacitors have been suggested using power loss index (PLI) for optimal sizing and location of capacitor. The optimal locations of flexible AC transmission systems (FACTS) devices have been determined based on voltage sensitivity index (VSI) of the system [27]. The line VSI and fast VSI have been obtained to reduce search space for location of FACTS in [28]. Various security based indices have been proposed for optimal reconfiguration [29].

In [30], VSI methods has been proposed for optimal location and sizing of DG. The monetary value of VSI has been improved [31] and the multi-objective function has been expressed to consolidate the static VSI for allocation of DG units [32]. Active and reactive PLIs have been proposed to find the best probable location of DG in [33]. An analytical approach associated with PLI for sizing and siting of DGs has been proposed in [34].

In [35], the multi objective performance index has been presented, and index vector method has been used for DG placement [36]. A new composite index of reliability of supply in the industrial systems with DG has been introduced in [37]. Reliability based indices and load point index have been proposed for optimal placement of DG [6].

However, less focus is given to find index for OPAS of APF. The numbers of APFs, its placement, size, and cost have been found by optimization algorithms in the existing literature. Therefore, the optimization algorithm takes the entire burden of finding the buses for placement as well as size of APF. For OPAS of APF considering NLDG, a nonlinear load position based APF current injection (NLPCI) technique has been proposed in [23]. In this paper an extension of NLPCI – ENLPCI is proposed. The placement and number of APFs are found using ENLPCI. This way, ENLPCI reduces the burden of the optimization algorithm. The optimization algorithm has to find the size only. It is very simple and accurate. The optimal placement for APF is calculated here for three distinct cases: a) only one state for minimum number of APFs, b) more than one state with different total harmonic distortion in voltage (THDv) with the same number of APFs and c) more than one state with the same THDv with the same number of APFs. It is well explained and formulated in Section 2.7.2.

GWO is recognized as one of the most modern bio-inspired algorithms due to its simplicity and flexibility [38,39]. It has very less parameters and exploration and exploitation property with the right balance [40]. Many electrical engineering power system problems have been effectively solved by GWO. In [41], a harmonic estimator has been designed using GWO. A new MPPT has been designed using GWO in [42]. Optimal tuning of multi-machine power system stabilizers has been done by utilizing GWO in [43]. The optimal allocation of the microgrid problem has been addressed by GWO in [44]. Moreover, the variants of GWO [39] have also gained more attention from researchers because of efficient results. An intelligent GWO has been developed and applied for bidding in energy market [45]. Improved leadership based GWO has been used in [46] for optimal coordination of overcurrent relays. Improved GWO has been utilized for optimal operation of a hydropower plant in [47]. Quasi-oppositional GWO has been used for load frequency control in [48]. In [49], novel hybrid GWO-SCA has been proposed for optimization problems. A nonconvex economic load dispatch problem has been solved by hybrid GWO in [50]. A modified GWO has been utilized for AGC [51] and improved energy production in wind plant [52]. A novel DE-GWO has been utilized for damping for power system oscillations in [53]. The adaptive differential search algorithm was used for optimal location of DG in [33]. An adaptive gravitational search algorithm has been utilized for optimal setting of FACTS devices in [27]. To improve the performance of cuckoo search algorithm (CSA), an adaptive technique has been used [54]. In [55], adaptive CSA (ACSA) has been used for better performance of CSA. AGWO has been implemented in [56] to detect partial discharge. As per No-Free-Lunch' theorem, there is always a scope for improvement in optimization [57], which motivates authors to use the adaptive version of GWO – AGWO in this paper.

The main contributions of this paper considering the OPAS of APF with the integration of NLDG and nonlinear load are as under:

- During the day, the variability of NLDG is analyzed and incorporated in the OPAS of APF problem.
- A novel ENLPCI technique is developed to find the OPAS for APFs while leaving only the size and cost of the APF to be determined by the optimization algorithm.
- AGWO is used for the optimal sizing of APF. It improves the cost of APF compared to GWO.

The next section of this paper represents the problem formulation, including the execution of ENLPCI, AGWO for OPAS of APF. Simulation results analysis are discussed next. Finally paper ends with the conclusion.

2. Problem formulation

This section describes the mathematical formulation of RDS with nonlinear loads, NLDGs and APFs. Each component of this system is modeled, and harmonic load flow along with optimization is described in detail. Fig. 1 shows the RDS with nonlinear loads, NLDGs and APFs. The process is as follows:

2.1. RDS modeling

The branch impedance of RDS (Zb) is described as

$$Zb = Rb + jXb \tag{1}$$

$$Zb^{(h)} = Rb + jXb^{(h)} \tag{2}$$

$$Xb^{(h)} = \omega_h Lb \tag{3}$$

$$\omega_h = 2\pi f_h \tag{4}$$

where, h denotes the order of harmonics, Rb and Lb represent resistance and inductance of branch, respectively, ω_h and f_h are angular harmonic frequency and harmonic frequency, respectively.

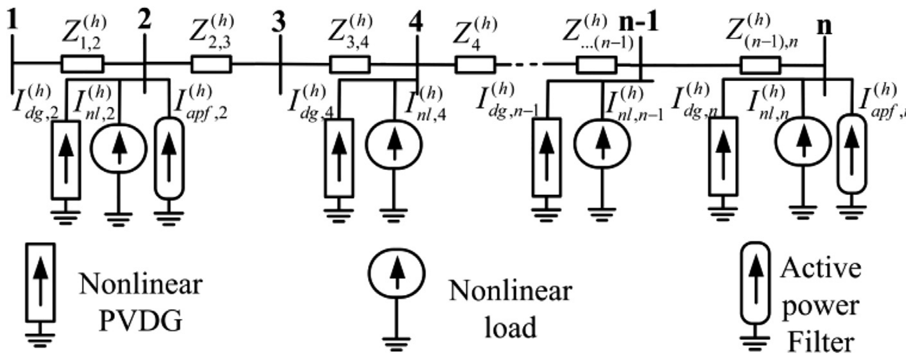

Fig. 1. RDS with Nonlinear loads, NLDGs and APFs.

2.2. Nonlinear load modeling

The representation of nonlinear load can be formulated by keeping the source of harmonic current injection as the base, as shown in [14,21]. The magnitude of rms nonlinear current can be calculated as

$$I_{nl}^{(h)} = I_{nl,r}^{(h)} + jI_{nl,im}^{(h)} \tag{5}$$

$$I_{nl} = \left[\sum_{h=2}^{H}\left(I_{nl,r}^{2(h)} + I_{nl,im}^{2(h)}\right)\right]^{1/2} \tag{6}$$

Here, $I_{nl,r}^{(h)}$ is the real part of a nonlinear current, while $I_{nl,im}^{(h)}$ is the imaginary part of nonlinear current, I_{nl} indicates the rms value, the highest order of harmonics is H.

2.3. DG modeling

The DG, a current source [1,58], supplies the harmonics in the system. The fundamental current is estimated [1] by the power rating of the DG, and therefore, NLDG harmonic current is calculated from the spectrum as below:

$$I_{hdg}^{(h)} = K_{dg}I_{dg} \tag{7}$$

Here, $I_{hdg}^{(h)}$, K_{dg} and I_{dg} are the harmonic current of NLDG, part of the harmonic current, and the fundamental current of DG, respectively.

2.4. APF modeling

APF is represented as a current source [14–17,20,21,59,60]. The calculation of I_{apf} is done on the basis of net nonlinear current (I_{nldg}). Net nonlinear current is a vector addition of nonlinear currents of loads and NLDGs. When the phase angle is zero, the distortion is worst as the net nonlinear current is a function of phase angle. So it causes maximum distortion while harmonic currents are in phase;

$$I_{nldg}^{(h)} = I_{hdg}^{(h)} + I_{nl}^{(h)} \tag{8}$$

$$I_{apf} = k(I_{nldg}) \tag{9}$$

Here, k is proportionate of net nonlinear current. It has the value such that I_{apf} satisfies the constraints.

APF is represented as a set of current sources. It injects harmonics order at a point of common coupling (PCC) as per the value of k. The APF current is expressed as,

$$I_{apf}^{(h)} = I_{apf,r}^{(h)} + jI_{apf\ ,im}^{(h)} \tag{10}$$

$$I_{apf} = \left[\sum_{h=2}^{H}\left(I_{apf,r}^{2(h)} + I_{apf,im}^{2(h)}\right)\right]^{1/2} \tag{11}$$

Here, $I_{apf,r}^{(h)}$, $I_{apf,im}^{(h)}$ and I_{apf} the real part, imaginary part and the rms value of current of APF respectively.

2.5. Modeling of solar power generation

The output power of solar panels is proportional to irradiance. In [24,61], the mean value of hourly solar irradiance and data regarding solar panels is given. From this data, the output power of a solar power plant is calculated as under:

$$P_{pv}(si) = \eta^{pv} \times S^{pv} \times si \tag{12}$$

where, P_{pv} is output power in kW for irradiancesi, η^{pv} is efficiency (%), S^{pv} total area of PV *in* m^2.

To generate the samples of the output power of a solar power plant, normal probability density function is used [62,63]. The mean value of solar irradiance and using (12), the 50,000 samples are generated each hour of output power and to deal with this, is a challenging task. To reduce computational time, the data should be reduced. Here, k-means scenario reduction algorithm [64,65] is utilized to reduce the number of samples from 50,000 to 100. It is used to arrange the original scenarios of solar irradiation into the clusters according to similarities. The reduced samples of output of solar power are used to calculate the harmonic currents injected by NLDG. These harmonic currents distort the voltage of the system.

2.6. Harmonic load flow

In this paper, network topology based harmonic load flow is used [66]. In which, two matrices are formed *viz.* a) bus injection to branch current (BIBC) and b) branch current to the bus voltage (BCBV). Then it is coupled with the optimization algorithm. THDv is calculated at all the buses using harmonic load flow. It is essential for the identification of critical buses that violate the standard limits. The THD_V is given as

$$THDv = \frac{\sqrt{\sum_{h=2}^{H}(IHDv)^2}}{V_f^1} \tag{13}$$

Here, V_f^1 is a fundamental frequency voltage.

From the value of THDv at all buses, the vital buses where the IEEE standard limits are not satisfied are found. It helps to decide the policy to alleviate the harmonics, i.e., the placement and sizing of APF.

2.7. Optimization process

The OPAS of APF is a nonlinear constraint optimization problem. This optimization process consists of an objective function, variables, and constraints. Here, the objective function has been formulated with constraints. The minimization of cost of harmonic filters is the main objective. The cost of APF is directly proportional to its current rating. Therefore, it is essential to reduce the current of APF such that all the constraints are fulfilled.

2.7.1. Objective function

The objective function is formulated on the basis of the total cost of APF required for harmonic mitigation. Total APF current ($I_{apf,Nft}$) is calculated for Nft APFs as

$$I_{apf,Nft} = \sum_{nft=1}^{Nft} I_{apf} \tag{14}$$

The total cost of APF is separated into two parts: a) fixed cost and b) incremental cost. The fixed cost is according to the number of units of APFs, and it is assumed as U.S. $ 90,000/unit, and incremental cost is based on the current compensated by APF, and it is assumed as U.S. $ 7,20,000/unit current [16,67]. The incremental cost of APF is given as,

$$C_{INC} = 7,20,000 \times I_{apf,Nft} \tag{15}$$

The total cost is given as,

$$Cost_{apf} = (No.\,of\,APF_S \times 90,000) + C_{INC} \tag{16}$$

The objective function is a function of current of APF, fixed, and incremental cost of APF. It is illustrated as,

$$OF_{TC} = \min Cost_{apf} + DP \tag{17}$$

Such that $THDv \leqslant 5\%, IHDv \leqslant 3\%,$ and $I_{apf} \leqslant I_{apf,\,max}$.

Where, DP is a dynamic penalty and $I_{apf,max}$ is the maximum current of APF.

The THDv and IHDv are controlled by the IEEE standard 519, and the maximum current of APF is limited by the total nonlinear current. For the constraint handling dynamic penalty is used is here. It gives the penalty according to the violation of the standard limit. If constraints are fulfilled, the penalty becomes zero otherwise it becomes high. It discards the infeasible solution from the final solution. The ENLPCI, GWO, and AGWO found the location for APF with its rating, such that the cost of APF is minimized.

2.7.2. ENLPCI formulation

In this section, ENLPCI is formulated. Extended NLPCI is proposed here to find the optimal buses for placement of APF in RDS. The proposed technique consists of three cases: a) only one feasible state with a minimum number of APF, b) more than one state with same number of APFs with different THDv, and c) more than one state with same number of APF and same THDv. In [23], the NLPCI technique has been introduced to decide the feasible buses for the entire 33-bus RDS. This technique is extended here and formulated as follows:

Create the nonlinear load position based APF placement matrix:

The total number of nonlinear load is denoted by NL and its buses is denoted by B_{NL}.

Then nonlinear loads are represented as,

$$1, \ldots, \ldots, \ldots, \ldots, NL \tag{18}$$

The nonlinear load buses are represented as,

$$1, \ldots, \ldots, \ldots, \ldots, B_{NL} \tag{19}$$

The nonlinear load position based matrix is formed and possible combinations of APFs placement are calculated. Each combination comprises of a set of nonlinear load buses and it is denoted by state St. Number of total state ST is determined from nonlinear load buses as,

$$ST = 2^{NL} - 1 \tag{20}$$

The nonlinear load position based APF placement combination matrix is formed as,

$$ST = 2^{NL} - 1 \quad \begin{array}{c|cccccc|c} \text{State} & 1 & 2 & \cdots & B_{NL}-1 & B_{NL} & & \text{Number of APF} \\ St_1 & 1 & 0 & \cdots & 0 & 0 & & 1 \\ St_2 & 0 & 1 & \cdots & 0 & 0 & & 1 \\ \vdots & \vdots & \vdots & \cdots & \vdots & \vdots & & \vdots \\ St_n & 1 & 0 & \cdots & 0 & 1 & & n \\ \vdots & \vdots & \vdots & \vdots & \vdots & \vdots & & \vdots \\ ST-1 & 1 & 1 & \cdots & 1 & 0 & & Nft-1 \\ ST & 1 & 1 & 1 & 1 & 1 & & Nft \end{array} \tag{21}$$

Here, '1' represents the placement of APF and '0' represents no APF.

Form the set of feasible states SF:

APF with an equal rating of the nonlinear load is connected at possible combination i.e., each state. Then THDv is calculated at all the buses using harmonic load flow for all the states. According to their maximum THDv the states are denoted as,

$$St_{1THD_V max}, \ldots\ldots, \ldots\ldots, ST_{THD_V max} \tag{22}$$

Separation of feasible and infeasible state is done by fulfilling the standard limit of THDv as,

$$State\,St \in \left\{ \begin{array}{c} SF,\ St_{THD_V max} \leqslant 5\% \\ Infeasible,\ St_{THD_V max} > 5\% \end{array} \right\} \tag{23}$$

Form the group according to the number of APFs:

All the states are arranged as per their number of filters. Here, the total nonlinear load buses are NL. Therefore the maximum possible combination according to the number of APFs is decided by NLC_{Nft}.

The group is formed as,

$$\begin{array}{lll} G_1 & \{SF_1 \ \cdots \ SF_{NLC_1}\} & (Group\ with\ one\ filter) \\ G_2 & \{SF_2 \ \cdots \ SF_{NLC_2}\} & (Group\ with\ two\ filters) \\ \vdots & \left\{ \vdots \quad \cdots \quad \vdots \right\} & \\ G_{Nft} & \{SF_{Nft}\} & (Group\ with\ maximum\ filters) \end{array} \tag{24}$$

The group with the maximum number of APFs has only one state.

Find the group with minimum filters:

$$G_{Nft,\min}\{SF_{1,Nft,\min} \ \cdots \ SF_{NL}C_{Nft,\min}\} \tag{25}$$

Sort the states of the above group according to their THDv:

$$G_{Nft,\min}\{SF_{1,Nft,\min,THDv,\min} \ \cdots \ SF_{NL}C_{Nft,\min}, THDv, \max\} \tag{26}$$

Prepare a table of priority rank of nonlinear load buses:

Find the THDv of a particular nonlinear load bus when only one APF is placed at the same node. Repeat the same process for all nonlinear loads and corresponding buses. Sort these buses as per their THDv – from the lowest THDv to the highest THDv. Give the 1st rank to a bus, that has the lowest THDv and vice versa for a bus that has the highest THDv.

The proposed ENLPCI is summarized in step by step as follows:

Read the data- line and load data, location of nonlinear loads and NLDGs with its rating and harmonic spectrum.
Select the nonlinear load buses from given data.
Form the nonlinear load position based matrix using (20) and (21).
Calculate I_{nl} from (6) for all nonlinear loads.
Place APFs at nonlinear load buses with an equal rating of I_{nl} for all the states.
Run harmonic load flow and calculate THDv at all the buses using (13) for all states.
Find the maximum THDv for all states using (22).
Determine the feasible states from all states according to their maximum THDv using (23).
Form the groups of feasible states according to the number of APF using (24).
Select the group which has a minimum number of APF/APFs using (25). If this group contains only one state, than this state is an optimal state for placement of APF and proceeds for the optimal size. Otherwise, the next step is used to find the optimal state.
In this step, the states are sorted according to their THDv using (26). In this case, if only one state is found, then it is considered as an optimal state. For more than one state with the same THDv, step 12 is used.
Select the state which has buses with higher priority rank. This state is an optimal state for APF placement and proceeds further for the optimal sizing of APF. The flowchart of the proposed ENLPCI is shown in Fig. 2.

AGWO is implemented to find the size and cost of APF at all buses found by ENLPCI which is described in the next section.

2.7.3. AGWo

To improve the results, the AGWO is used here. The randomization has an important role in the exploration and the exploitation of metaheuristic optimization techniques. Some of the techniques for randomization are Markov chain, levy flights, and Gaussian or normal distribution, and adaptive. In adaptive technique, the step size changes adaptively towards the optimal solution considering the best fitness value and worst fitness value throughout iteration. It results in fast convergence. The step size is given as [56],

$$Ss^{(t+1)} = \left(\frac{1}{t}\right)^{((bestft(t)-fit(t))/(bestft(t)-worstft(t))} \tag{27}$$

where, Ss is the step size, t is iteration, $bestft$ is the best fitness, fit is fitness and $worstft$ is the worst fitness.

In the proposed algorithm, the position of the grey wolf is mapped as the cost of APF. It is coupled with harmonic load flow to find the best fitness-cost of APF and is considered as alpha (α) score. The corresponding variables are stored as α position. In the same way, the second and third best solutions are stored and named – beta (β) and delta (δ), respectively. According to the best fit, the search agents revise their positions. It is repeated for all iterations.

The step by step procedure to apply AGWO is given below:

Total iterations (T), Total run (N_{run}), numbers of grey wolves (N_{gwa}) are set.
The cost of the APF is initialized randomly. As per the grey wolves initial positions, the position matrix at t^{th} iteration is created as,

$$\vec{C}ost_{apf,pos}(t) = \begin{bmatrix} \vec{C}ost^1_{apf,1} & \vec{C}ost^1_{apf,2} & \cdots & \vec{C}ost^1_{apf,Nft-1} & \vec{C}ost^1_{apf,Nft} \\ \vec{C}ost^2_{apf,1} & \vec{C}ost^2_{apf,2} & \cdots & \vec{C}ost^2_{apf,Nft-1} & \vec{C}ost^2_{apf,Nft} \\ \vdots & \vdots & \cdots & \vdots & \vdots \\ \vec{C}ost^{Ngwa-1}_{apf,1} & \vec{C}ost^{Ngwa-1}_{apf,2} & \cdots & \vec{C}ost^{Ngwa-1}_{apf,Nft-1} & \vec{C}ost^{Ngwa-1}_{apf,Nft} \\ \vec{C}ost^{Ngwa}_{apf,1} & \vec{C}ost^{Ngwa}_{apf,2} & \cdots & \vec{C}ost^{Ngwa}_{apf,Nft-1} & \vec{C}ost^{Ngwa}_{apf,Nft} \end{bmatrix} \tag{28}$$

The cost of APF for all grey wolves is calculated using (17).

$$Cost_{apf}(t) = \left[Cost_{apf1}, Cost_{apf2}, \cdots, Cost_{apfNgwa-1}, Cost_{apfNgwa}\right]^T \tag{29}$$

After sorting from the lowest to the highest value of fitness of the above matrix (29) the classification of the scores and positions of α, β, and δ is done as,

1st best solution represents α score $\vec{C}ost_{apf,\alpha,score}(t)$ and the corresponding position is $\vec{C}ost_{apf,\alpha,pos}(t)$ (30)

2nd best solution represents β score $\vec{C}ost_{apf,\beta,score}(t)$ and the corresponding position is $\vec{C}ost_{apf,\beta,pos}(t)$ (31)

3rd best solution represents δ score $\vec{C}ost_{apf,\delta,score}(t)$ and the corresponding position is $\vec{C}ost_{apf,\delta,pos}(t)$ (32)

The obtained solutions of α, β, and δ are compared with previous solutions (solutions at (t − 1)th iteration) and updated as:

$$\vec{C}ost_{apf,\alpha,score}(t) = \left\{ \begin{array}{c} \vec{C}ost_{apf,\alpha,score}(t-1),\ if\ \vec{C}ost_{apf,\alpha,score}(t) > \vec{C}ost_{apf,\alpha,score}(t-1) \\ \vec{C}ost_{apf,\alpha,score}(t),\ if\ \vec{C}ost_{apf,\alpha,score}(t) \leqslant \vec{C}ost_{apf,\alpha,score}(t-1) \end{array} \right\} \tag{33}$$

$$\vec{C}ost_{apf,\beta,score}(t) = \left\{ \begin{array}{c} \vec{C}ost_{apf,\beta,score}(t-1),\ if\ \vec{C}ost_{apf,\beta,score}(t) > \vec{C}ost_{apf,\beta,score}(t-1) \\ \vec{C}ost_{apf,\beta,score}(t),\ if\ \vec{C}ost_{apf,\beta,score}(t) \leqslant \vec{C}ost_{apf,\beta,score}(t-1) \end{array} \right\} \tag{34}$$

$$\vec{C}ost_{apf,\delta,score}(t) = \left\{ \begin{array}{c} \vec{C}ost_{apf,\delta,score}(t-1),\ if\ \vec{C}ost_{apf,\delta,score}(t) > \vec{C}ost_{apf,\delta,score}(t-1) \\ \vec{C}ost_{apf,\delta,score}(t),\ if\ \vec{C}ost_{apf,\delta,score}(t) \leqslant \vec{C}ost_{apf,\delta,score}(t-1) \end{array} \right\} \tag{35}$$

Same way in $(t+1)$th iteration

$$\vec{C}ost_{apf,\alpha,score}(t+1) = \left\{ \begin{array}{c} \vec{C}ost_{apf,\alpha,score}(t),\ if\ \vec{C}ost_{apf,\alpha,score}(t+1) > \vec{C}ost_{apf,\alpha,score}(t) \\ \vec{C}ost_{apf,\alpha,score}(t+1),\ if\ \vec{C}ost_{apf,\alpha,score}(t+1) \leqslant \vec{C}ost_{apf,\alpha,score}(t) \end{array} \right\} \tag{36}$$

$$\vec{C}ost_{apf,\beta,score}(t+1) = \left\{ \begin{array}{c} \vec{C}ost_{apf,\beta,score}(t),\ if\ \vec{C}ost_{apf,\beta,score}(t+1) > \vec{C}ost_{apf,\beta,score}(t) \\ \vec{C}ost_{apf,\beta,score}(t+1),\ if\ \vec{C}ost_{apf,\beta,score}(t+1) \leqslant \vec{C}ost_{apf,\beta,score}(t) \end{array} \right\} \tag{37}$$

$$\vec{C}ost_{apf,\delta,score}(t+1) = \left\{ \begin{array}{c} \vec{C}ost_{apf,\delta,score}(t),\ if\ \vec{C}ost_{apf,\delta,score}(t+1) > \vec{C}ost_{apf,\delta,score}(t) \\ \vec{C}ost_{apf,\delta,score}(t+1),\ if\ \vec{C}ost_{apf,\delta,score}(t+1) \leqslant \vec{C}ost_{apf,\delta,score}(t) \end{array} \right\} \tag{38}$$

The encircling and hunting behavior of the grey wolves have been proposed in [38]. In this, the position of (ij)th grey wolf

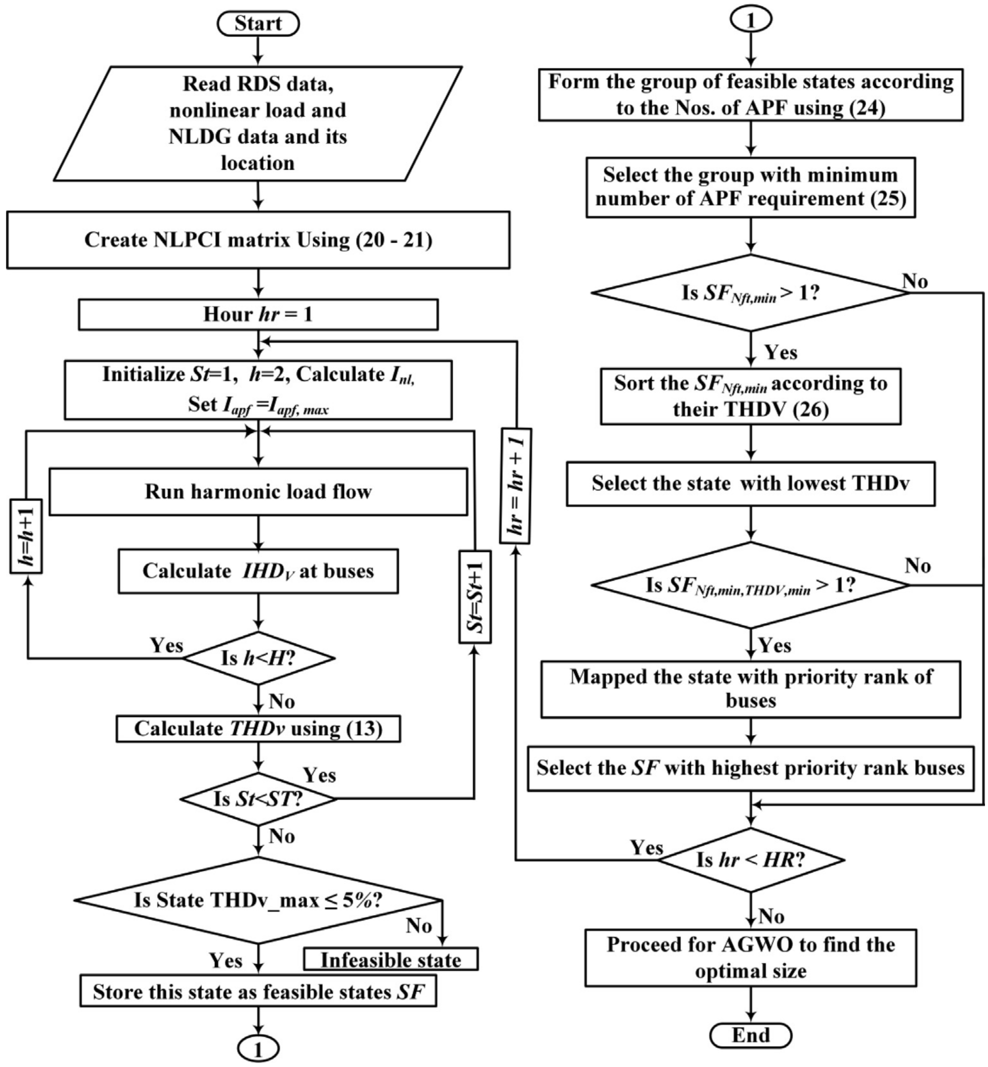

Fig. 2. Flow chart for ENLPCI.

is revised according to the position of α as$\vec{M}_{\alpha,ij} = \left|\vec{B}_{\alpha,ij} * \vec{C}ost_{apf,\alpha,pos,j}(t) - \vec{C}ost_{apf,pos,ij}(t)\right|$ (39)

$$\vec{Y}_{\alpha,ij} = \vec{C}ost_{apf,\alpha,pos,j}(t) - \vec{S}_{\alpha,ij} * \vec{M}_{\alpha,ij} \tag{40}$$

$$\vec{s}(t) = 2 - t * (2/T) \tag{41}$$

$$\vec{S}_{\alpha,ij} = 2 * \vec{s}(t) * \vec{r}_{1\alpha,ij} - \vec{s}(t) \tag{42}$$

$$\vec{B}_{\alpha,ij} = 2 * \vec{r}_{2\alpha,ij} \tag{43}$$

where, i = 1, 2,. . .,. . .,$N_{gwa} - 1$, N_{gwa}, and j = 1, 2,. . .,. . ..,$Nft - 1$, Nft. Here, i and j represent the row and column of matrix respectively, t indicates current iteration, $\vec{r}_{1\alpha,ij}$ and $\vec{r}_{2\alpha,ij}$ are the random vectors in [0, 1], $\vec{S}_{\alpha,ij}$ and $\vec{B}_{\alpha,ij}$ are the coefficients vectors in terms of α and elements of $\vec{s}$ are linearly decreased from [0, 1] during the iterative process and half of the iterations are devoted to exploration phase and rest are for exploitation phase.

Similarly, the position of (ij)th grey wolf is revised according to the position of β and δ and it is expressed as

$$\vec{M}_{\beta,ij} = \left|\vec{B}_{\beta,ij} * \vec{C}ost_{apf,\beta,pos,j}(t) - \vec{C}ost_{apf,pos,ij}(t)\right| \tag{44}$$

$$\vec{Y}_{\beta,ij} = \vec{C}ost_{apf,\beta,pos,j}(t) - \vec{S}_{\beta,ij} * \vec{M}_{\beta,ij} \tag{45}$$

$$\vec{M}_{\delta,ij} = \left|\vec{B}_{\delta,ij} * \vec{C}ost_{apf,\delta,pos,j}(t) - \vec{C}ost_{apf,pos,ij}(t)\right| \tag{46}$$

$$\vec{Y}_{\delta,ij} = \vec{C}ost_{apf,\delta,pos,j}(t) - \vec{S}_{\delta,ij} * \vec{M}_{\delta,ij} \tag{47}$$

where, $\vec{S}_{\beta,ij}$ and $\vec{B}_{\beta,ij}$ are the coefficients vectors in terms of β, $\vec{S}_{\delta,ij}$ and $\vec{C}_{\delta,ij}$ are the coefficients vectors in terms of δ.

Now, the revised value of APF cost for (t + 1)th iteration is given as

$$\vec{C}ost^{i}_{apf,j}(t+1) = \frac{\vec{Y}_{\alpha,ij} + \vec{Y}_{\beta,ij} + \vec{Y}_{\delta,ij}}{3} \tag{48}$$

Update the grey wolves position using (48).
Update the position of all grey wolves using adaptive equation (27).
Go to step 2 until T.

The updated cost – $\vec{C}ost_{apf,\alpha,score}$ is the optimum cost of APF.

AGWO is implemented as shown in Fig. 3. The simulation results are discussed in the next section.

3. Simulation results and discussion

This part is devoted to the simulation results and discussion.

3.1. System data

In this paper, IEEE-69 bus [68] test system as shown in Fig. 4 is considered for simulation. Here, the NLDG supplies the nonlinear loads is assumed. All nonlinear loads have the same harmonic spectrum as per six pulse converter [69]. Harmonic contents of NLDG is shown in Fig. 5 [70]. The nonlinear loads are located at buses 27, 35, 46, 50, 52, 65, 67, and 69. i.e., at all end nodes. End nodes are selected to observe the severe effect of harmonics on the entire RDS.

3.2. Results and discussion

As stated in problem formulation section, the NLDG generates power according to the solar irradiance during the day time from hour 6 to hour 19. Therefore, the power supplied to the nonlinear loads is also different for each hour, which results in different levels of harmonics injected by nonlinear loads for each hour. In the morning and evening periods, the solar irradiance is less so the power supplied to the nonlinear loads is also less. It results in less harmonics distortion. But solar irradiance is more in the noon period. Therefore harmonics are more in the noon period. To fulfill the IEEE standard, control of harmonics in the RDS is required. Here, the harmonics level is not constant and so it is not easy to control. In the available literature, the harmonics level is assumed to be constant because of the constant load. So the calculation of THDv is done for only one load. Due to consideration of variable nonlinear load, THDv is calculated for each hour.

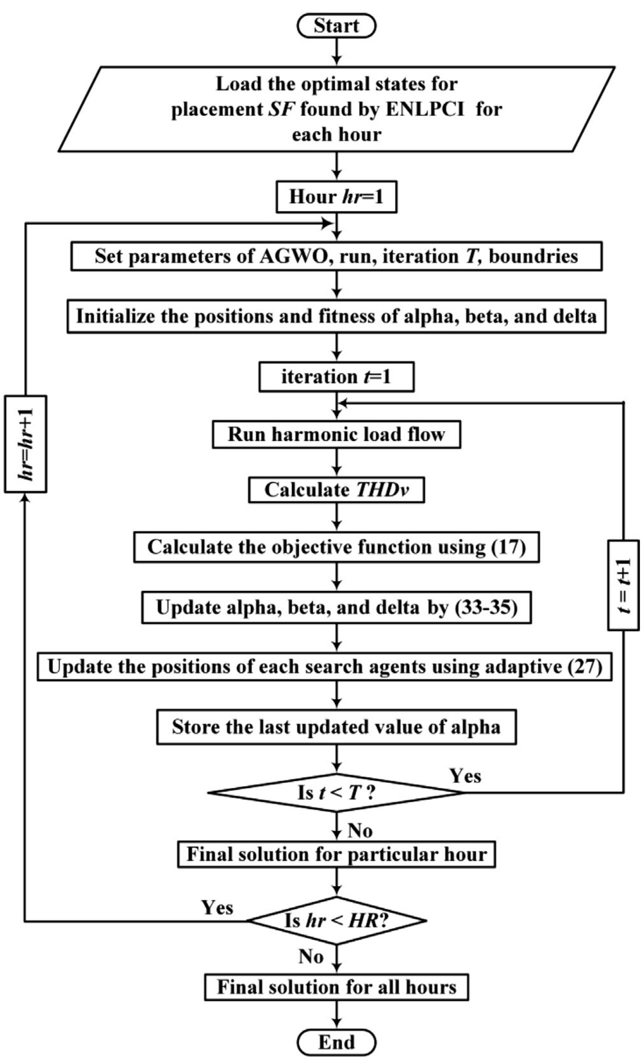

Fig. 3. Flow chart for implementing AGWO for OPAS of APF.

APF is used to mitigate the harmonics and maintain the standard limits. A simple solution to control the harmonics in RDS with NLDG and nonlinear load is to place the APF at all the harmonics polluted load nodes. Here, eight buses have harmonics polluted loads, therefore without any calculation APFs are placed at all eight buses which have nonlinear loads and NLDGs, i.e. (buses 27, 35, 46, 50, 52, 65, 67 and 69). This easy solution is very costly because the eight APFs with a current rating of same as harmonics injected by NLDGs and nonlinear loads are required. Therefore, an optimization technique is needed to solve this problem.

The ENLPCI technique, GWO and AGWO are used here to find the OPAS of APF. For the optimization process, algorithms run for 10 times with 40 numbers of search agents and 100 iterations.

The harmonic distortion at all the buses is tabulated in Table 1 for hour 12. Among 69 buses, only 16 buses have THDv less than 5%; rest 52 buses have crossed the standard limit. The highest THDv is 49.95% at bus 27. It is seen that the RDS is highly polluted at hour 12. It is also noticed that the highest THDv is calculated at bus 27 for all hours. So bus 27 has the prime importance in the placement of APF.

Figs. 6–9 depicts the THDv at all 69 buses for each hour (from hour 7 to hour 18). It is observed that during the initial hour, the THDv is less compared to the noon period. For hour 6 and hour 19, the maximum THDv is less than 5%. From hour 7 to hour 18 it is, 6.14, 14.17, 27.42, 37.95, 47.10, 49.95, 48.50, 44.19, 35.04, 24.20, 12.16, and 5.09 (THDv is in %), respectively. In this section, the harmonic pollution condition at all the buses for all hours is discussed. In the next section, the selection of optimal buses using ENLPCI is described

3.3. ENLPCI

Here, eight buses have nonlinear loads and NLDGs is considered. Therefore, a total of 255 ($2^8 - 1 = 255$) possible combinations for APF placement are formed as per the nonlinear load position matrix [23]. Each combination is represented as a state and exhaustive results are taken. Using (20) and (21) the 255 rows by 8 columns matrix is generated. After that, for each state at all 68 buses, THDv is calculated. Feasible states are found among these 255 states by (22). Among them, the optimal placement of the APF is found by ENLPCI for each hour. It is an accurate method. The optimal buses found by the ENLPCI are also verified by optimization algorithms. At the infeasible buses, the optimization algorithms are not converged, while vice versa for feasible buses. Table 2 represents the number of states with the number of APFs.

The number of feasible states found for one day by ENLPCI is tabulated in Table 3. The lowest THDv_maximum found at hour 18 compared with other hours and observed that it has the highest feasible states-248. At hours 12 and 13, the feasible state is only one; it is due to a high THDv_maximum. Rest of the hours has feasible states according to the THDv_maximum.

3.3.1. ENLPCI case 1

From Table 3, it is noticed that for hours 10 to 15 only one feasible state is available for a particular number of APFs. i.e., for seven APFs, the feasible state is one and the same for eight APFs. In this case, the state with the minimum number of APFs is considered to be the optimal state.

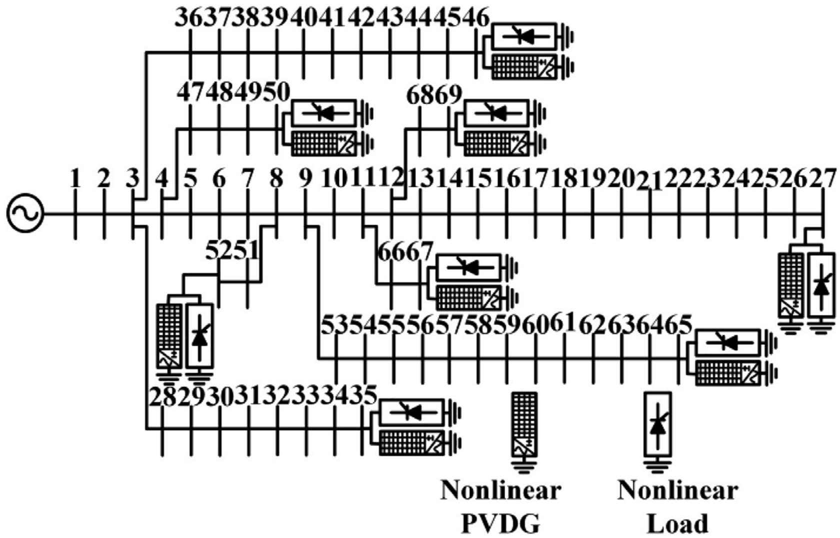

Fig. 4. IEEE 69-bus distribution system with nonlinear loads and NLDGs.

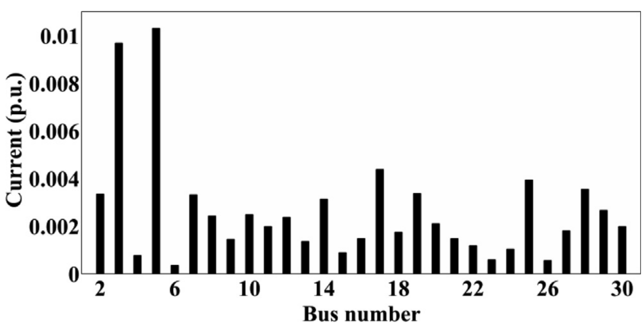

Fig. 5. Harmonic contents of NLDG at hour 12.

Table 4 represents the comparison of feasible states with number of APFs found by ENLPCI and AGWO. Table 5, represents the case 1. The optimal buses found by ENLPCI are also validated by AGWO.

The current of APF for this state is minimum compared to all other states for a particular hour.

Fig. 10 compares the best fitness curve between GWO and AGWO for hour 11 wherein it is observed that the AGWO converged fast compared to GWO. The AGWO found lower value of cost ($1,025,958) compared to the cost found by GWO ($1,032,177). It proves the efficacy of AGWO for OPAS of APF.

3.3.2. ENLPCI case-2

For the remaining time period, the scenario is different. i.e., at hour 9 feasible state numbers are 248, 250, and 255. Among them for 248 and 250 states, seven APFs are required. This indicates that after providing seven APFs, THDv is within the standard limit at all buses in the entire IEEE-69 RDS. But the question is that how to select the optimal state from these feasible sates? It is solved by ENLPCI technique. The least THDv for a given feasible state is preferred for the optimal state. Therefore, at hour 9, the most feasible sate for seven APFs is 250 because it has the least THDv 2.84% compared to 4.04% THDv of state 248. It is also validated by GWO and AGWO. The size of APFs found by optimization algorithms is more in the case of state 248 compared to state 250. Table 6 shows the results of ENLPCI for different time periods for case 2.

An interesting fact is that the above ENLPCI results are also supported by Table 7- the priority rank of buses. This table is formed by giving priority to the buses according to their THDv found by ENLPCI for each hour. The bus which has the lowest THDv for a given state has the highest priority and vice versa for a bus with the highest THDv. It is sorted from the lowest THDv to the highest

Table 1
THDv (%) at all buses in the absence of filter at hour 12.

Bus No.	THDv (%)	Bus No.	THDv (%)	Bus No.	THDv (%)	Bus No.	THDv (%)
2	0.08	19	**43.56**	36	0.25	53	**20.81**
3	0.16	20	**44.14**	37	1.53	54	**21.66**
4	0.33	21	**45.08**	38	2.54	55	**22.86**
5	1.54	22	**45.12**	39	2.83	56	**24.05**
6	**9.26**	23	**45.57**	40	2.85	57	**28.52**
7	**17.29**	24	**46.53**	41	**9.83**	58	**30.73**
8	**19.24**	25	**48.61**	42	**12.80**	59	**31.57**
9	**20.07**	26	**49.47**	43	**13.19**	60	**32.56**
10	**26.88**	27	**49.95**	44	**13.29**	61	**34.70**
11	**28.44**	28	0.25	45	**14.42**	62	**35.11**
12	**32.39**	29	1.53	46	**14.43**	63	**35.72**
13	**35.25**	30	2.62	47	0.40	64	**38.72**
14	**38.11**	31	2.82	48	2.11	65	**43.11**
15	**41.04**	32	3.79	49	**7.92**	66	**28.96**
16	**41.59**	33	**6.15**	50	**9.57**	67	**28.97**
17	**42.63**	34	**10.90**	51	**19.63**	68	**34.45**
18	**42.64**	35	**14.99**	52	**20.59**	69	**34.46**

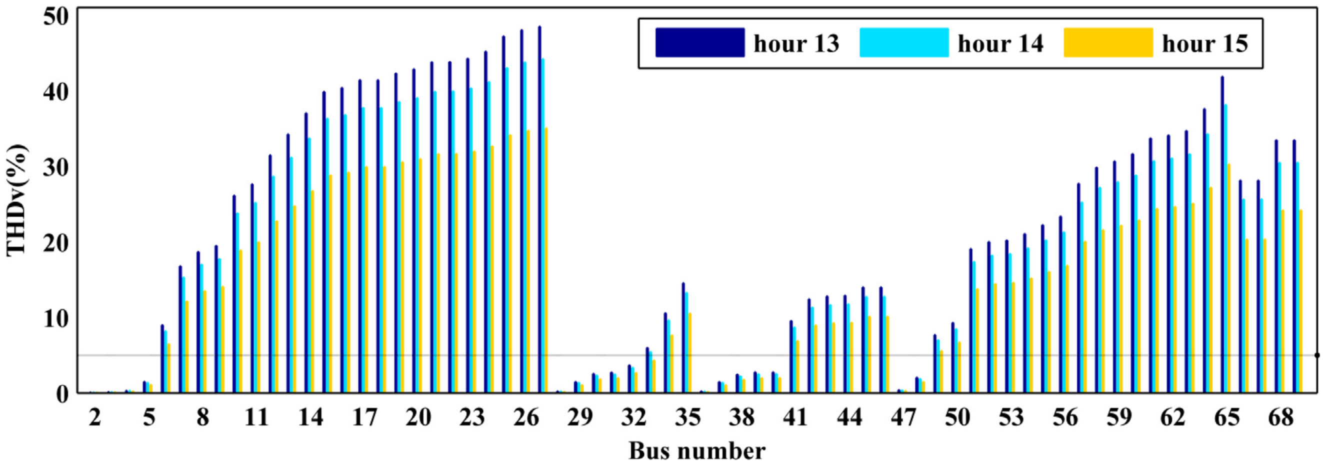

Fig. 6. THDv at all buses for hour 7 to hour 9.

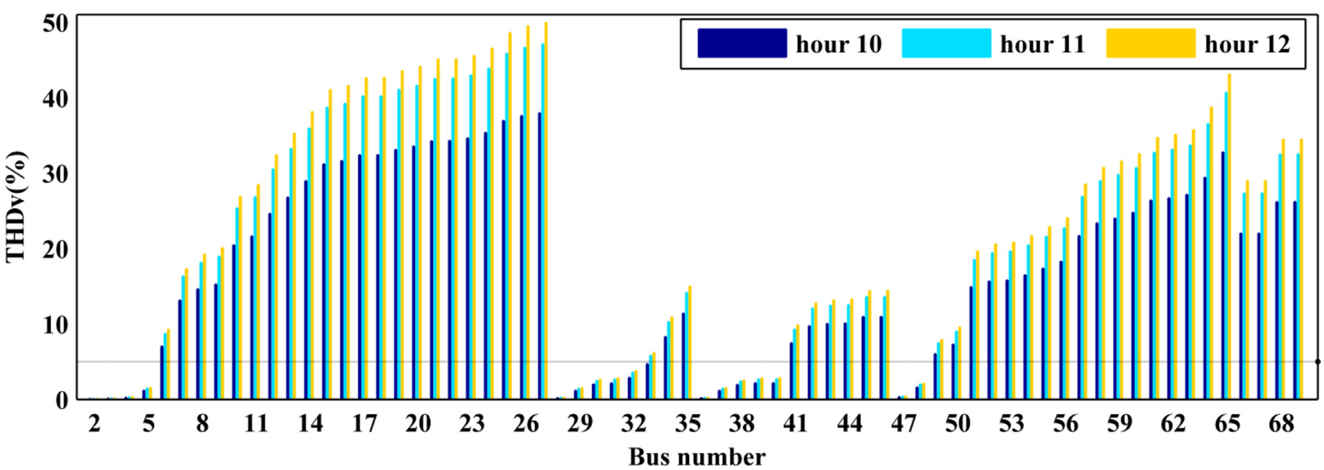

Fig. 7. THDV at all buses for hour 10 to hour 12.

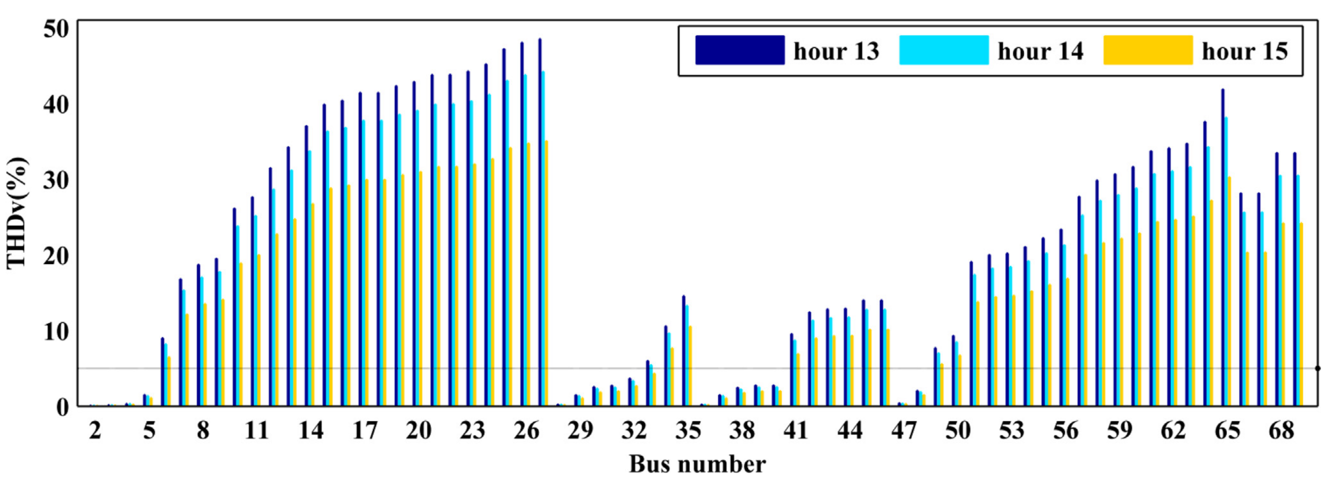

Fig. 8. THDv at all buses for hour 13 to hour 15.

THDv and tabulated in Table 7. The priority rank of buses remains the same for all hours. At hour 9, the only difference is that in the state 250, bus 67 is present while in the state 248, bus 52 is present. Other buses remain the same in both states. Bus 67 has the higher priority than bus 52 and hence the optimal placement is state 250.

At hour 18, there are five feasible states with one APF as given in Table 6 – 1, 5, 6, 7, and 8. State 1 has the lowest THDv, so it is the

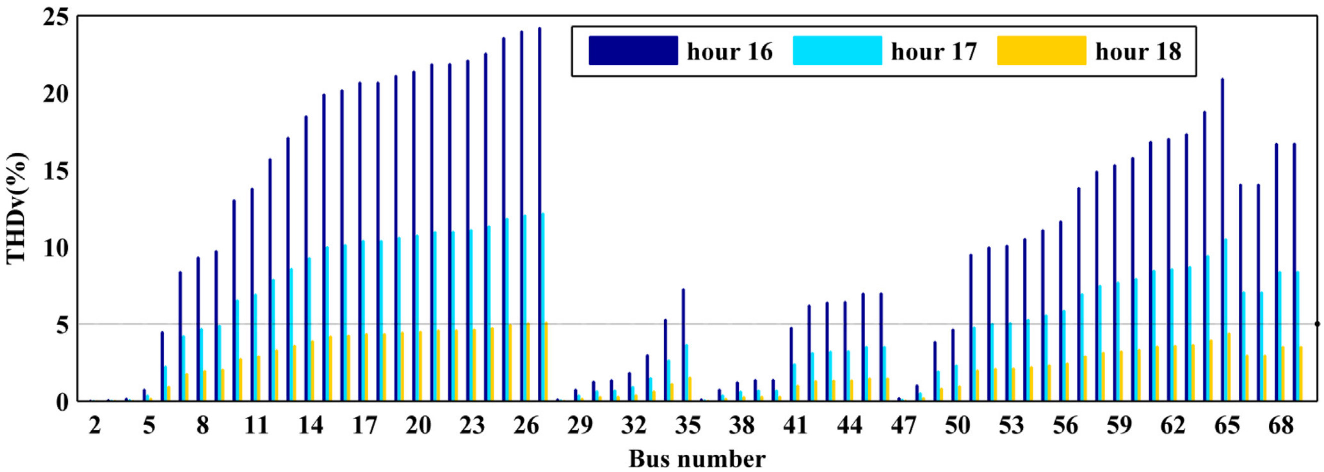

Fig. 9. THDV at all buses for hour 16 to hour 18.

Table 2
Number of APF for different states by ENLPCI.

Number of APF	1	2	3	4	5	6	7	8
Number of states	$8C_1$	$8C_2$	$8C_3$	$8C_4$	$8C_5$	$8C_6$	$8C_7$	$8C_8$
State number	1–8	9–36	37–92	93–162	163–218	219–246	247–254	255

Table 3
The feasible states with number of APFs for different hours by ENLPCI.

Hour	Number of APFs								Total feasible states
	1	2	3	4	5	6	7	8	
7	1	12	40	63	55	28	8	1	208
8	0	0	2	9	16	14	6	1	48
9	0	0	0	0	0	0	2	1	3
10	0	0	0	0	0	0	1	1	2
11	0	0	0	0	0	0	1	1	2
12	0	0	0	0	0	0	0	1	1
13	0	0	0	0	0	0	0	1	1
14	0	0	0	0	0	0	1	1	2
15	0	0	0	0	0	0	1	1	2
16	0	0	0	0	0	2	3	1	6
17	0	0	3	12	19	15	6	1	56
18	5	25	55	70	56	28	8	1	248

Table 4
Feasible States for different hours with number of APFs validated by AGWO.

Hour	Proposed ENLPCI				AGWO
	Total feasible states	Feasible state with minimum nos. of APFs & its (THDv_max (%))	Nos. of APFs	Optimal state	Optimal state
7	208	1 (4.80)	1	1	1
8	48	67 (4.24), 82 (4.24)	3	82	82
9	3	248 (4.04), 250 (2.84)	7	250	250
10	2	250 (3.93)	7	250	250
11	2	250 (4.88)	7	250	250
12	1	255	8	255	255
13	1	255	8	255	255
14	2	250 (4.58)	7	250	250
15	2	250 (3.63)	7	250	250
16	6	228 (4.52), 237 (4.52)	6	237	237
17	56	53 (4.33), 67 (3.64), 82 (3.64)	3	82	82
18	248	1 (3.98), 5 (4.7), 6 (4.68), 7 (4.39), 8 (4.19)	1	1	1

optimal state. It is proved by priority rank Table 7; it is clear that bus 27 has the highest priority among all buses. It is also validated by AGWO. The current of APF for different states is different as shown in Table 6. The state with a bus that has a higher priority as per Table 7 has less current.

3.3.3. ENLPCI case 3

Another provocation fact is that when THDv is the same for all the feasible states for the same number of APFs, which is the most suitable state? i.e., in Table 8, at hour 8 states 67 and 82, both have same number of APFs and THDv, same for hour 16 (states 228 and

Table 5
Case 1 – Only one state for a minimum number of APF.

Hour	State	Number of APF	APF Bus	THDv_max (%) as per ENLPCI	Optimal I_{apf} by AGWO
7	1	1	27	4.8	0.00757
10	250	7	27, 35, 46, 50, 65, 67, 69	3.93	0.39523
11	250	7	27, 35, 46, 50, 65, 67, 69	4.88	0.54994
12	255	8	27, 35, 46, 50, 52, 65, 67, 69	0.00	0.60566
13	255	8	27, 35, 46, 50, 52, 65, 67, 69	0.00	0.57298
14	250	7	27, 35, 46, 50, 65, 67, 69	4.58	0.50635
15	250	7	27, 35, 46, 50, 65, 67, 69	3.63	0.34865

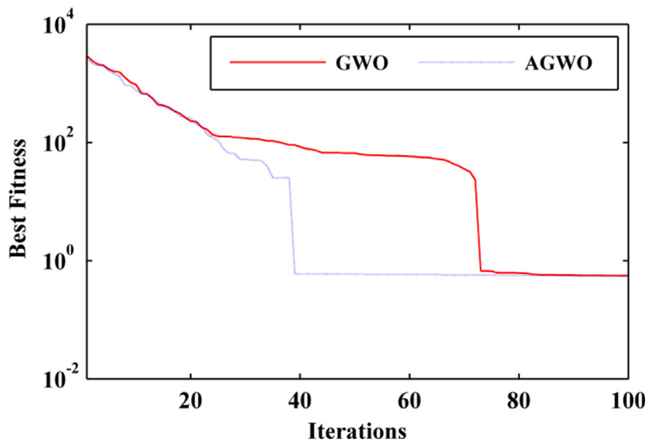

Fig. 10. Best fitness curve.

238). The solution of this is given by bus priority rank algorithm. The state has most prior buses compared to other states is selected as the most suitable state for placement of APFs.

At hour 8, in states numbers 67 and 82 have the same THDv. State 67 consists of buses – 27, 65, and 67. State 82 consists of buses – 27, 65, and 69. The common buses are 27 and 65. The different buses are 67 and 69. Bus 69 has the higher priority than bus 67. So, as per priority rank, state 82 is the optimal placement of APF which is validated in the last column of Table 8 by AGWO with a current of 0.06315 p.u. It is less compared to current found for state 67 – 0.06625 p.u.

At hour 16, the states – 228 and 237 have the same THDv – 4.52%. The difference in buses is 27 and 67. Bus no 67 has more priority than bus 52 as per Table 7. Therefore state 237 is the optimal placement of APF. AGWO found the less current of APF – 0.1828p.u. compared to state 228–0.18383p.u. as shown in the last column of Table 8. That is also same as for hour 17, the difference in buses is bus 67 and 69, so state 82 is the optimal placement of APF. The current of APF found by AGWO is 0.04634p.u. for state 82 compared to 0.04778p.u. for state 67.

Moreover, the results are verified with AGWO. The current for APF is found as per Table 8 and it is the strong evidence in support of validation of ENLPCI.

The results for each hour (i.e., hours 7 to 18) are summarized and compared in terms of current and cost with nonoptimized

Table 6
Case 2 – More than one state with different THDv with the same number of APF.

Hour	State	Number of APF	APF Bus	THDv_max (%) as per ENLPCI	Optimal I_{apf} by AGWO (p.u.)
9	248	7	27, 35, 46, 50, 52, 65, 69	4.04	0.23545
9	**250**	7	27, 35, 46, 50, 65, 67, 69	**2.84**	**0.23204**
18	**1**	1	27	**3.98**	**0.00034**
18	5	1	52	4.70	0.00231
18	6	1	65	4.68	0.00219
18	7	1	67	4.39	0.00129
18	8	1	69	4.19	0.00100

Table 7
Priority rank by ENLPCI.

Priority Rank	1	2	3	4	5	6	7	8
State no.	1	8	7	6	5	4	2	3
Bus no.	27	69	67	65	52	50	35	46

Table 8
Case 3 - More than one state with same THDv with same number of APF.

Hour	State	Number of APF	APF Bus	THDv_max (%) as per ENLPCI	Optimal Iapf by AGWO (p.u.)
8	67	3	27, 65, 67	4.24	0.06625
8	**82**	3	27, 65, 69	4.24	**0.06315**
16	228	6	27, 35, 46, 52, 65, 69	4.52	0.18383
16	**237**	6	27, 35, 46, 65, 67, 69	4.52	**0.18280**
17	67	3	27, 65, 67	3.64	0.04778
17	**82**	3	27, 65, 69	3.64	**0.04634**

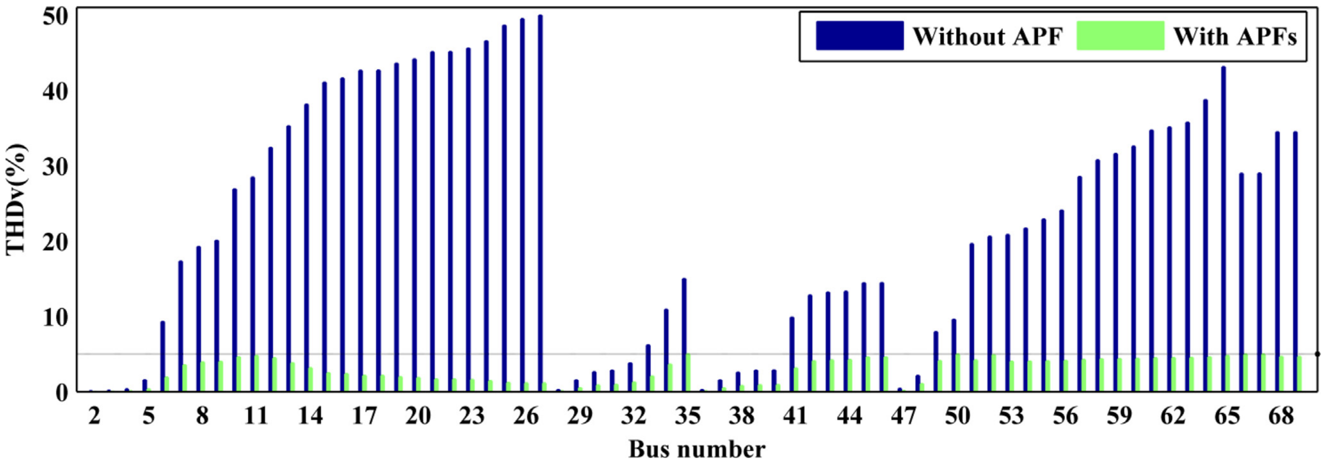

Fig. 11. THDv at different buses without APF and with APFs at hour 12.

Table 9
Summary and comparative value of APF current and cost for hours 7 to 12.

Hour	THDv max (%)	Nonoptimized value		Optimized value							
		I_{apf} (p.u.)	Total cost ($)	State as per ENLPCI	Nos. of APF	APF buses	Algorithm	I_{apf} (p.u.)	Total cost ($)	Saving compared to nonoptimized value (%)	Saving compared to GWO (%)
7	6.14	0.1000582	792,042	1	1	27	GWO	0.00756843	95,449	87.95	0.00
							AGWO	0.00756843	95,449	87.95	
8	14.17	0.2309162	886,260	82	3	27, 65, 69	GWO	0.06363602	315,818	64.37	0.11
							AGWO	**0.06315433**	**315,471**	64.40	
9	27.42	0.4468148	1,041,707	250	7	27, 35, 46, 50, 65, 67, 69	GWO	0.23226898	797,234	23.47	0.02
							AGWO	**0.23203989**	**797,069**	23.48	
10	37.95	0.6183704	1,165,227	250	7	27, 35, 46, 50, 65, 67, 69	GWO	0.40225842	919,626	21.08	0.55
							AGWO	**0.39522564**	**914,562**	21.51	
11	47.10	0.767414	1,272,538	250	7	27, 35, 46, 50, 65, 67, 69	GWO	0.55857877	1,032,177	18.89	0.60
							AGWO	**0.54994143**	**1,025,958**	19.38	
12	49.95	0.8138247	1,305,954	255	8	27, 35, 46, 50, 52, 65, 67, 69	GWO	0.61613346	1,163,616	10.90	0.65
							AGWO	**0.60565998**	**1,156,075**	11.48	

Table 10
Summary and comparative value of APF current and cost for hours 13 to 18.

Hour	THDv max (%)	Nonoptimized value		Optimized value							
		I_{apf} (p.u.)	Total cost ($)	State as per ENLPCI	Nos. of APF	APF buses	Algorithm	I_{apf} (p.u.)	Total Cost ($)	Saving compared to nonoptimized value (%)	Saving compared to GWO (%)
13	48.50	0.790301	1,289,017	255	8	27, 35, 46, 50, 52, 65, 67, 69	GWO	0.58835419	1,143,615	11.28	0.97
							AGWO	**0.57298029**	**1,132,546**	12.14	
14	44.19	0.7199737	1,238,381	250	7	27, 35, 46, 50, 65, 67, 69	GWO	0.51565911	1,001,275	19.15	0.67
							AGWO	**0.50635397**	**994,575**	19.69	
15	35.04	0.5710122	1,131,129	250	7	27, 35, 46, 50, 65, 67, 69	GWO	0.35085436	882,615	21.97	0.18
							AGWO	**0.34864998**	**881,028**	22.11	
16	24.20	0.3942998	1,003,896	237	6	27, 35, 46, 65, 67, 69	GWO	0.18414215	672,582	33.00	0.14
							AGWO	**0.18279882**	**671,615**	33.10	
17	12.16	0.1980979	862,631	82	3	27, 65, 69	GWO	0.04635914	303,379	64.83	0.00
							AGWO	**0.04634361**	**303,367**	64.83	
18	5.09	0.0828851	779,677	1	1	27	GWO	0.00033537	90,241	88.43	0.00
							AGWO	0.00033536	90,241	88.43	

solution in Tables 9 and 10. Nonoptimized solution means, eight APFs are placed at eight nonlinear load buses i.e. 27, 35, 46, 50, 52, 65, 67 and 69 with the same rating of nonlinear loads.

Here, for each hour the OPAS of APF is calculated. The saving in cost is the maximum at hour 18–88.43% compared to nonoptimized solution. At hour 12, the optimal cost of APF found by AGWO is $1,156,075. In this case, the saving is 11.48%. It is observed that AGWO performed better compared to GWO. It has found a better value of APF current for most of the hours. It results in lesser cost. The lowest cost is highlighted in bold.

Moreover, it is also observed that the requirement of number of APFs and its size to minimize the harmonic pollution to acceptable level is different for each hour. No APFs are required at hour 6 and hour 19. During this time period, all buses have THDv less than 5%. For another time period, there is a requirement of a different number of APFs. At hour 12, cost for a nonoptimized solution is $

1,305,954. Finally, it is reduced to $1,156,075 by AGWO. It is a significant saving in terms of cost which proves the necessity of ENLPCI and AGWO for OPAS of APF.

Fig. 11 shows the THDv at all buses at hour 12-without APF and with APFs. Without APF total of 52 buses have THDv more than the standard limit. It is noticed that without APF maximum THDv is 49.95% while after placing the eight APFs at buses 27, 35, 46, 50, 52, 65, 67, and 69, it is within a standard limit. AGWO found the lesser value of APF current and cost compared to GWO.

4. Conclusions

In this paper, a novel technique for OPAS of APF – ENLPCI is proposed and incorporated in the problem formulation for OPAS of APF using both GWO and AGWO. The problem of OPAS of APF is considered for the RDS with NLDGs. The effect of variability in harmonics due to the penetration of RES is accounted by an hourly analysis and solving the problem on an hourly basis. The optimal buses for the placement of APFs are found by ENLPCI and size of APF is optimized by GWO and AGWO. The AGWO performed better compared to GWO for all hours. The maximum cost saving is 88.43% at hour 18. The analysis considering hourly variable load is more prominent than considering only fixed load. For each hour the number of APFs, their placement and sizes are different. It proves the necessity to include the variable nonlinear load in the analysis. The analysis shows that the cost of the APFs varies between a minimum of $ 90,241 to a maximum of $ 1,156,075. Similarly, saving is from a maximum of 88% at hour 18 to a minimum 11.48% at hour 12 compared to a nonoptimal solution.

Declaration of Competing Interest

The authors declare that they have no known competing financial interests or personal relationships that could have appeared to influence the work reported in this paper.

References

[1] S. Sakar, M.E. Balci, S.H.A. Aleem, A.F. Zobaa, Increasing PV hosting capacity in distorted distribution systems using passive harmonic filtering, Electr. Power Syst. Res. 148 (2017) 74–86.
[2] N.R. Battu, A. Abhyankar, N. Senroy, DG planning with amalgamation of operational and reliability considerations, Int. J. Emerg. Electr. Power Syst. 17 (2016) 131–141.
[3] A. Uniyal, A. Kumar, Optimal distributed generation placement with multiple objectives considering probabilistic load, Procedia Comput. Sci. 125 (2018) 382–388.
[4] T. Ackermann, G. Andersson, L. Söder, Distributed generation: a definition, Electr. Power Syst. Res. 57 (2001) 195–204.
[5] P. Kayal, C. Chanda, Optimal mix of solar and wind distributed generations considering performance improvement of electrical distribution network, Renew. Energy 75 (2015) 173–186.
[6] G.H. Reddy, P. Chakrapani, A.K. Goswami, N.B.D. Choudhury, Optimal distributed generation placement in distribution system to improve reliability and critical loads pick up after natural disasters, Eng. Sci. Technol. Int. J. 20 (2017) 825–832.
[7] N. Gira, A.K. Dahiya, Solar PV-BES in distribution system with novel technique for DC voltage regulation, Eng. Sci. Technol. Int. J. 2020.
[8] V. Hengsritawat, T. Tayjasanant, N. Nimpitiwan, Optimal sizing of photovoltaic distributed generators in a distribution system with consideration of solar radiation and harmonic distortion, Int. J. Electr. Power Energy Syst. 39 (2012) 36–47.
[9] M.H. Bollen, R. Das, S. Djokic, P. Ciufo, J. Meyer, S.K. Rönnberg, et al., Power quality concerns in implementing smart distribution-grid applications, IEEE Trans. Smart Grid 8 (2016) 391–399.
[10] F. Wang, J.L. Duarte, M.A. Hendrix, P.F. Ribeiro, Modeling and analysis of grid harmonic distortion impact of aggregated DG inverters, IEEE Trans. Power Electron. 26 (2010) 786–797.
[11] IEEE Recommended Practice and Requirements for Harmonic Control in Electric Power Systems, IEEE, New York, NY, 2014.
[12] B. Singh, K. Al-Haddad, A. Chandra, A review of active filters for power quality improvement, IEEE Trans. Ind. Electron. 46 (1999) 960–971.
[13] L.R. Lima, F.N. Belchior, P.F. Ribeiro, A novel approach to the design of passive filters in electric grids, Int. J. Emerg. Electr. Power Syst. 17 (2016) 693–701.
[14] I. Ziari, A. Jalilian, A new approach for allocation and sizing of multiple active power-line conditioners, IEEE Trans. Power Delivery 25 (2010) 1026–1035.
[15] I. Ziari, A. Jalilian, Optimal allocation and sizing of active power line conditioners using a new particle swarm optimization-based approach, Electr. Power Compon. Syst. 40 (2012) 273–291.
[16] I. Ziari, A. Jalilian, Optimal placement and sizing of multiple APLCs using a modified discrete PSO, Int. J. Electr. Power Energy Syst. 43 (2012) 630–639.
[17] R. Keypour, H. Seifi, A. Yazdian-Varjani, Genetic based algorithm for active power filter allocation and sizing, Electr. Power Syst. Res. 71 (2004) 41–49.
[18] M. Farhoodnea, A. Mohamed, H. Shareef, H. Zayandehroodi, Optimum placement of active power conditioner in distribution systems using improved discrete firefly algorithm for power quality enhancement, Appl. Soft Comput. 23 (2014) 249–258.
[19] M. Farhoodnea, A. Mohamed, H. Shareef, H. Zayandehroodi, Optimum placement of active power conditioners by a dynamic discrete firefly algorithm to mitigate the negative power quality effects of renewable energy-based generators, Int. J. Electr. Power Energy Syst. 61 (2014) 305–317.
[20] M. Shivaie, A. Salemnia, M.T. Ameli, A multi-objective approach to optimal placement and sizing of multiple active power filters using a music-inspired algorithm, Appl. Soft Comput. 22 (2014) 189–204.
[21] M. Shivaie, A. Salemnia, M.T. Ameli, Optimal multi-objective placement and sizing of passive and active power filters by a fuzzy-improved harmony search algorithm, Int. Trans. Electr. Energy Syst. (2013).
[22] G. Carpinelli, D. Proto, A. Russo, Optimal planning of active power filters in a distribution system using trade-off/risk method, IEEE Trans. Power Delivery 32 (2017) 841–851.
[23] A. Lakum, V. Mahajan, Optimal placement and sizing of multiple active power filters in radial distribution system using grey wolf optimizer in presence of nonlinear distributed generation, Electr. Power Syst. Res. 173 (2019) 281–290.
[24] D.Q. Hung, N. Mithulananthan, K.Y. Lee, Determining PV penetration for distribution systems with time-varying load models, IEEE Trans. Power Syst. 29 (2014) 3048–3057.
[25] E. Kazemi-Robati, M.S. Sepasian, Passive harmonic filter planning considering daily load variations and distribution system reconfiguration, Electr. Power Syst. Res. 166 (2019) 125–135.
[26] A. Abdelaziz, E. Ali, S. Abd Elazim, "Optimal sizing and locations of capacitors in radial distribution systems via flower pollination optimization algorithm and power loss index, Eng. Sci. Technol. Int. J. 19 (2016) 610–618.
[27] S.R. Inkollu, V.R. Kota, Optimal setting of FACTS devices for voltage stability improvement using PSO adaptive GSA hybrid algorithm, Eng. Sci. Technol. Int. J. 19 (2016) 1166–1176.
[28] A. Sadiq, S. Adamu, M. Buhari, Optimal distributed generation planning in distribution networks: a comparison of transmission network models with FACTS, Eng. Sci. Technol. Int. J. 22 (2019) 33–46.
[29] B. Mahdad, Optimal reconfiguration and reactive power planning based fractal search algorithm: a case study of the Algerian distribution electrical system, Eng. Sci. Technol. Int. J. 22 (2019) 78–101.
[30] V.V. Murty, A. Kumar, Optimal placement of DG in radial distribution systems based on new voltage stability index under load growth, Int. J. Electr. Power Energy Syst. 69 (2015) 246–256.
[31] S. Nojavan, M. Jalali, K. Zare, An MINLP approach for optimal DG unit's allocation in radial/mesh distribution systems take into account voltage stability index, Iran. J. Sci. Technol. Trans. Electr. Eng. 39 (2015) 155–165.
[32] A. El-Fergany, Multi-objective allocation of multi-type distributed generators along distribution networks using backtracking search algorithm and fuzzy expert rules, Electr. Power Compon. Syst. 44 (2016) 252–267.
[33] B. Mahdad, K. Srairi, Adaptive differential search algorithm for optimal location of distributed generation in the presence of SVC for power loss reduction in distribution system, Eng. Sci. Technol. Int. J. 19 (2016) 1266–1282.
[34] R. Viral, D.K. Khatod, An analytical approach for sizing and siting of DGs in balanced radial distribution networks for loss minimization, Int. J. Electr. Power Energy Syst. 67 (2015) 191–201.
[35] N. Mohandas, R. Balamurugan, L. Lakshminarasimman, Optimal location and sizing of real power DG units to improve the voltage stability in the distribution system using ABC algorithm united with chaos, Int. J. Electr. Power Energy Syst. 66 (2015) 41–52.
[36] D.P.R.P.V. Veera, R.T. Gowri, Application of Flower Pollination algorithm for optimal, Electr. Power Energy Syst. 43 (2016) 1296–1304.
[37] R.M. Ciric, N.L. Rajakovic, A new composite index of reliability of supply in the industrial systems with distributed generation, Int. J. Electr. Power Energy Syst. 44 (2013) 824–831.
[38] S. Mirjalili, S.M. Mirjalili, A. Lewis, Grey wolf optimizer, Adv. Eng. Softw. 69 (2014) 46–61.
[39] H. Faris, I. Aljarah, M.A. Al-Betar, S. Mirjalili, Grey wolf optimizer: a review of recent variants and applications, Neural Comput. Appl. 30 (2018) 413–435.
[40] B. Dey, S.K. Roy, B. Bhattacharyya, Solving multi-objective economic emission dispatch of a renewable integrated microgrid using latest bio-inspired algorithms, Eng. Sci. Technol. Int. J. 22 (2019) 55–66.
[41] A. Saxena, R. Kumar, S. Mirjalili, A harmonic estimator design with evolutionary operators equipped grey wolf optimizer, Expert Syst. Appl. 145 (2020) 113125.
[42] S. Mohanty, B. Subudhi, P.K. Ray, A new MPPT design using grey wolf optimization technique for photovoltaic system under partial shading conditions, IEEE Trans. Sustain. Energy 7 (2016) 181–188.

[43] P. Dhanaselvi, S. S. Reddy, R. Kiranmayi, Optimal tuning of multi-machine power system stabilizer parameters using grey wolf optimization (GWO) Algorithm, in: Emerging Trends in Electrical, Communications, and Information Technologies, Springer, 2020, pp. 347–355

[44] J. Zhang, X. Wang, L. Ma, An optimal power allocation scheme of microgrid using grey wolf optimizer, IEEE Access 7 (2019) 137608–137619.

[45] A. Saxena, B.P. Soni, R. Kumar, V. Gupta, Intelligent Grey Wolf Optimizer-Development and application for strategic bidding in uniform price spot energy market, Appl. Soft Comput. 69 (2018) 1–13.

[46] S. Gupta, K. Deep, Optimal coordination of overcurrent relays using improved leadership-based grey wolf optimizer, Arab. J. Sci. Eng. (2019) 1–11.

[47] Z.-K. Feng, S. Liu, W.-J. Niu, Y. Liu, B. Luo, S.-M. Miao, et al., Optimal operation of hydropower system by improved grey wolf optimizer based on elite mutation and quasi-oppositional learning, IEEE Access 7 (2019) 155513–155529.

[48] D. Guha, P.K. Roy, S. Banerjee, Load frequency control of large scale power system using quasi-oppositional grey wolf optimization algorithm, Eng. Sci. Technol. Int. J. 19 (2016) 1693–1713.

[49] N. Singh, S. Singh, A novel hybrid GWO-SCA approach for optimization problems, Eng. Sci. Technol. Int. J. 20 (2017) 1586–1601.

[50] M.A. Al-Betar, M.A. Awadallah, M.M. Krishan, A non-convex economic load dispatch problem with valve loading effect using a hybrid grey wolf optimizer, Neural Comput. Appl. (2019) 1–28.

[51] S. Padhy, S. Panda, S. Mahapatra, A modified GWO technique based cascade PI-PD controller for AGC of power systems in presence of Plug in Electric Vehicles, Eng. Sci. Technol. Int. J. 20 (2017) 427–442.

[52] M.M. Tumari, M.H. Suid, M.A. Ahmad, A modified Grey Wolf Optimizer for improving wind plant energy production, Indonesian J. Electr. Eng. Comput. Sci. 18 (2020) 1123–1129.

[53] N. Nahak, R.K. Mallick, Damping of power system oscillations by a novel DE-GWO optimized dual UPFC controller, Eng. Sci. Technol. Int. J. 20 (2017) 1275–1284.

[54] P. Ong, Adaptive cuckoo search algorithm for unconstrained optimization, Sci. World J. 2014 (2014).

[55] M.K. Naik, R. Panda, A novel adaptive cuckoo search algorithm for intrinsic discriminant analysis based face recognition, Appl. Soft Comput. 38 (2016) 661–675.

[56] K. Dudani, A. Chudasama, Partial discharge detection in transformer using adaptive grey wolf optimizer based acoustic emission technique, Cogent Eng. (2016).

[57] D.H. Wolpert, W.G. Macready, No free lunch theorems for optimization, IEEE Trans. Evol. Comput. 1 (1997) 67–82.

[58] S. Sakar, M.E. Balci, S.H.A. Aleem, A.F. Zobaa, Integration of large-scale PV plants in non-sinusoidal environments: considerations on hosting capacity and harmonic distortion limits, Renew. Sustain. Energy Rev. 82 (2018) 176–186.

[59] H.-C. Chang, T.-T. Chang, Optimal installation of three-phase active power line conditioners in unbalanced distribution systems, Electr. Power Syst. Res. 57 (2001) 163–171.

[60] A. Moradifar, H.R. Soleymanpour, A fuzzy based solution for allocation and sizing of multiple active power filters, J. Power Electron. 12 (2012) 830–841.

[61] M. Mazidi, A. Zakariazadeh, S. Jadid, P. Siano, Integrated scheduling of renewable generation and demand response programs in a microgrid, Energy Convers. Manage. 86 (2014) 1118–1127.

[62] M. Aien, M.G. Khajeh, M. Rashidinejad, M. Fotuhi-Firuzabad, Probabilistic power flow of correlated hybrid wind-photovoltaic power systems, IET Renew. Power Gener. 8 (2014) 649–658.

[63] S.S. Reddy, Optimal scheduling of thermal-wind-solar power system with storage, Renew. Energy 101 (2017) 1357–1368.

[64] L. Baringo, A. Conejo, Correlated wind-power production and electric load scenarios for investment decisions, Appl. Energy 101 (2013) 475–482.

[65] I. Khan, J.Z. Huang, M.A. Masud, Q. Jiang, Segmentation of factories on electricity consumption behaviors using load profile data, IEEE Access 4 (2016) 8394–8406.

[66] J.-H. Teng, S.-H. Liao, R.-C. Leou, Three-phase harmonic analysis method for unbalanced distribution systems, Energies 7 (2014) 365–384.

[67] Y. Zhao, H. Deng, J. Li, D. Xia, Optimal planning of harmonic filters on distribution systems by chance constrained programming, Electr. Power Syst. Res. 68 (2003) 149–156.

[68] M.E. Baran, F.F. Wu, Optimal capacitor placement on radial distribution systems, IEEE Trans. Power Delivery 4 (1989) 725–734.

[69] E. Fuchs, M.A. Masoum, Power Quality in Power Systems and Electrical Machines, Academic press, 2011.

[70] A.R. Oliva, J.C. Balda, A PV dispersed generator: a power quality analysis within the IEEE 519, IEEE Trans. Power Delivery 18 (2003) 525–530.